Thermo-Fluid Modeling of a Full Scale Liquid Hydrogen Storage System with Integrated Refrigeration

J. H. Baik[1], W. U. Notardonato[2], S. Karng[3], S. Kim[3], and I. Oh[4]

[1] Florida Solar Energy Center, University of Central Florida
Cocoa, FL, USA 32922

[2] Cryogenics Test Laboratory, Kennedy Space Center, FL, USA 32899

[3] Center for Urban Energy System Research, Korea Institute of Science Technology, Seoul, Korea 136791

[4] Green City Technology Institute, Korea Institute of Science Technology
Seoul, Korea 136791

ABSTRACT

Distribution of liquid hydrogen (LH_2) via tanker trucks is the most direct path towards meeting the delivery requirements in the early phases of the transition to a hydrogen-based energy economy. This will use larger, centralized production and liquefaction systems and tankers to deliver liquid to the distribution stations. Due to the low storage temperature, heat leak into the storage vessel will create boil off and pressurization and may eventually lead to venting and loss of product. Engineers at the NASA Kennedy Space Center have been dealing with these issues on a large scale since the 1960's with a normal evaporation rate on their 850,000 gallon LH_2 tanks varying between 600-1,000 gallons per day. The NASA KSC is currently developing a Ground Operations Demonstration Unit (GODU) for LH_2, where advanced operations including an integrated cryogenic refrigerator designed to remove heat from the stored liquid will be tested. This will allow for zero-loss storage and transfer operations, as well as control of the propellant state to enable conditioning or densification. The NASA KSC has partnered with the Florida Solar Energy Center to develop a thermo-fluid model of the integrated refrigeration and storage system to predict its behavior under a variety of operating conditions. This model will consider the thermo-physical properties and specifications of the associated fluids and materials in the GODU so as to achieve a more accurate prediction of behaviors. This paper discusses details of the GODU LH_2 system and the modeling parameters.

INTRODUCTION

Background

NASA's contribution to the development of the large scale LH_2 industry has been considerable through various space launch-vehicle programs such as the Apollo and the Space Shuttle programs. From the last several decades of launch operations at the KSC Launch Complexes,

Cryocoolers 18, edited by S.D. Miller and R.G. Ross, Jr.

cryogenic technology has significantly progressed in refrigeration systems, cryogen transfer, gas compression, system controls, and instrumentation. However, spaceport hydrogen operations are quite different from those of general industrial gas customers, and the industry is not optimized to meet spaceport's needs due to its large scale, unsteady/irregular demand, and the NASA's strict delivery requirements to the spaceport. A recent report on the historical average loss of LH_2 through the entire Space Shuttle Program indicates that the overall LH_2 loss is about 46% of the total purchased fuel.[1] This includes in-transit losses, chill-down of the transfer system, tanker pressurization, in-the-ground storage tank losses, chill-down of ground and flight system, and the external tank replenishment. The NASA acknowledged goal for a future spaceport is for technology that increases the efficiency of hydrogen operations to higher than 80%. This would focus on reducing storage tank boil-off and chill-down losses, improving recovery of tanker venting, and working on transfer line drain and purge, tank venting, local hydrogen production and liquefaction capability, and propellant conditioning and densification.

Recently, the KSC initiated the Integrated Ground Operations Demonstration Units (GODU) for the LH_2 project with participation from the Ames Research Center, the Glenn Research Center and the Stennis Space Center. The objectives of the project are to investigate alternative storage and distribution architectures for future cryogenic propellant operations, and to demonstrate advanced cryogenic propellant handling operations of normal boiling point (NBP) and subcooled cryogenic hydrogen.

GODU LH_2

The GODU LH_2 is based on the principle that hydrogen losses can be eliminated by integrating a refrigeration system into the storage tank. An oversized refrigerator would allow for propellant densification and in situ liquefaction by placing a cold heat exchanger in the LH_2 storage tank.[2-4] This active refrigeration concept has been successfully demonstrated at the Florida Solar Energy Center[5] and the Korea Institute of Science and Technology (KIST)[6] as a laboratory scale hydrogen liquefaction and densification operation using a cryocooler. The proposed GODU LH_2 will expand the scale and operations of the FSEC and the KIST demonstrations to larger scales in refrigeration power and storage volume. The main objective of the GODU LH_2 is to demonstrate zero loss storage and transfer of LH_2 at a large scale using a close cycle helium refrigerator, hydrogen densification in the storage tank, low-helium usage operations, and loading of flight tanks. The GODU LH_2 consists of a reverse-Brayton helium refrigerator (Linde R1620), the 33,000 gallon horizontal cylindrical storage tank with a modified manway for heat exchanger and instrumentation feed-through, the 'whale skeleton' structured heat exchanger, vacuum jacketed transfer lines, gaseous hydrogen venting and flare system, and LH_2 vaporizer.[3-4] Figure 1 shows a photo and schematics of the GODU LH_2 at the Hydrogen Technology Demonstration Site at the KSC.

Several modeling analyses have been performed of the cold heat exchanger and the thermal behavior of the LH_2 in the storage tank to provide heat exchanger design and system operation parameters for the GODU LH_2.[2-4] Now, the major interests of the GODU LH_2 researchers are: (1) thermal losses of the storage tank, (2) the thermodynamic condition of the LH_2 in the storage tank during liquefaction and densification, and (3) the transient behavior of two-phase hydrogen in the storage tank to predict operation time and fluid condition during liquefaction and densification. A lumped thermal and fluid modeling analysis on the storage tank has been performed for the liquefaction and densification mode based on the storage tank dimensions and the refrigerator performance. This paper explains details of the thermal modeling analyses and discusses their results.

THERMAL MODELING ANALYSIS

The current modeling analysis focuses on overall thermodynamic conditions of gaseous and liquid hydrogen during transient states such as in situ liquefaction and densification rather than detailed fluid dynamic behaviors of hydrogen in the tank and at its walls. The following assumptions were made for the modeling to simplify the analysis, interpretation of results, and prediction of the macroscopic fluid condition.

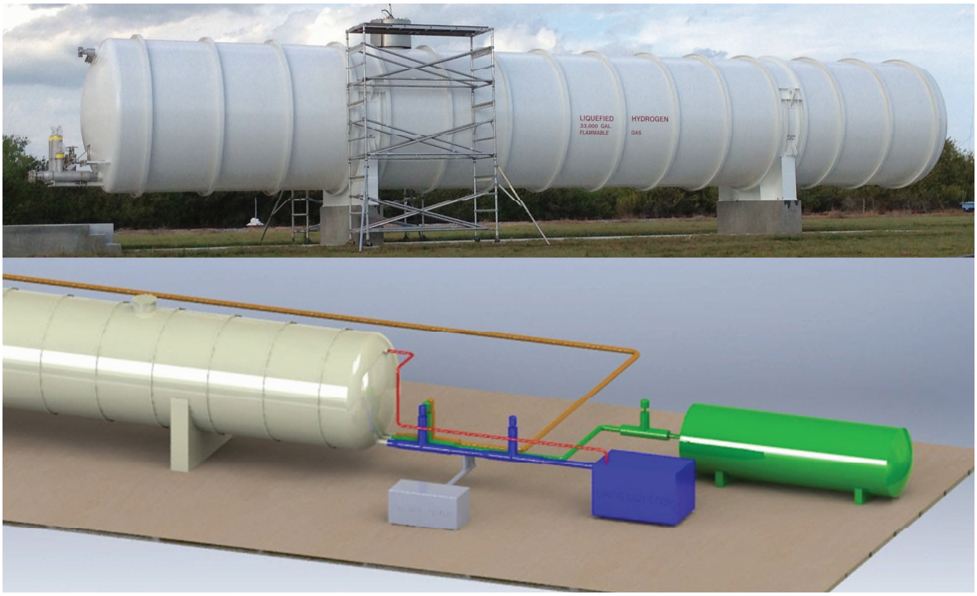

Figure 1. The GODU LH_2 at the Hydrogen Technology Demonstration Site at the NASA KSC.

For liquefaction mode:

a. Pressures of both gaseous and liquid hydrogen are equal, and remain constant.
b. Gaseous hydrogen flowing into the tank is precooled to 78 K with LN_2.
c. Temperature of gaseous hydrogen in the gas region is uniform, and remains constant at 78 K.
d. Temperature of liquid hydrogen in the liquid region is uniform, and is saturation temperature at given liquefaction pressure.
e. Mass transfer at gas-liquid surface is negligible compared to condensation at heat exchanger surface.
f. Condensation efficiency at the heat exchanger surface is ideal.

For densification mode,

a. Pressures of both gaseous and liquid hydrogen are equal, but varies over time.
b. There is no gaseous hydrogen flowing into the tank.
c. Temperature of gaseous hydrogen in the gas region is uniform, and remains constant at 50K.
d. Temperature of liquid hydrogen in the liquid region is uniform, and is saturation temperature at given densification pressure.
e., f. are the same as for the liquefaction mode.

The uniform fluid temperature assumption becomes reasonably valid for the quasi-equilibrium state where liquefaction time is on the order of days rather than seconds or minutes. Locally heated fluid near the walls travels upward by natural convection and moves to the center of the tank, and then gets cooled by the heat exchanger that is located in both the gas and liquid region. For this case of having heat sinks (heat exchangers) in the storage tank with a particularly large liquefaction time, the local thermal stratification effect can be ignored in our modeling.

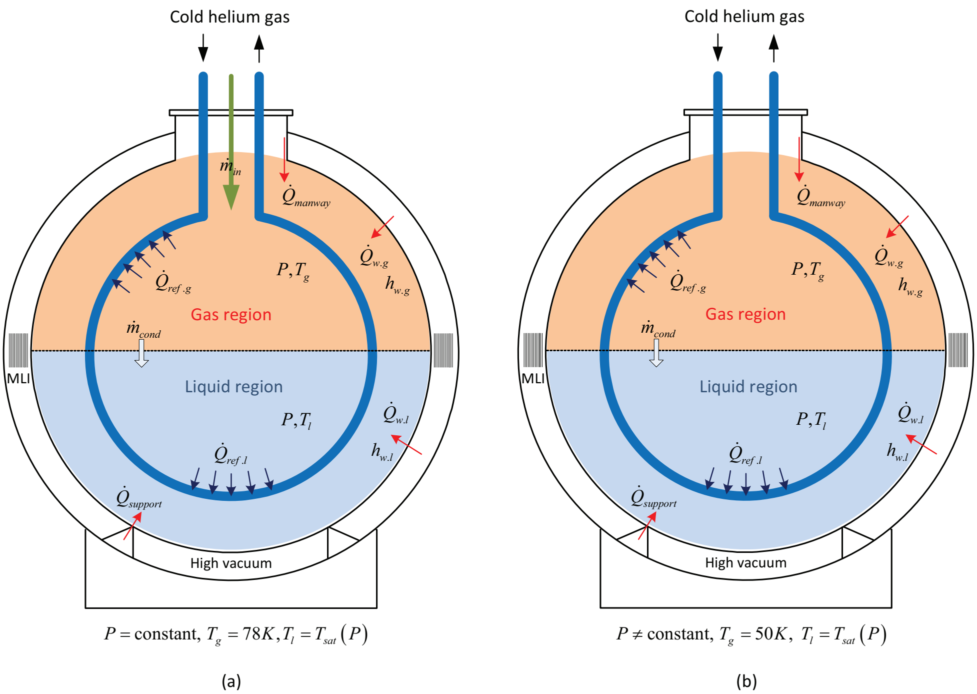

Figure 2. Schematics of a simplified lumped thermal model of the storage tank for (a) liquefaction and (b) densification mode.

Thermal Losses

Fig. 2 shows schematics of a simplified lumped thermal model of the storage tank for liquefaction and densification mode. For the storage tank that is partially filled with gaseous and liquid hydrogen, total heat leaks to the storage tank can be divided into four subcategories or routes: (1) heat leak through the tank wall in the gaseous hydrogen region($\dot{Q}_{w.g}$), (2) heat leak through the tank wall in the liquid hydrogen region($\dot{Q}_{w.l}$), (3) heat leak through manway and instrumentation ($\dot{Q}_{manway}$), and (4) heat leak through the inner tank supports and supply/drain line penetrations ($\dot{Q}_{support}$). The heat leaks through the tank walls that are wetted with gaseous and liquid hydrogen can be estimated by combination of natural convection heat transfer at near walls, conduction heat transfer through the wall, and multilayer insulation specification. The heat leaks through the manway and supports/line penetrations were previously estimated[3] as $\dot{Q}_{manway}$ = 50 W and $\dot{Q}_{support}$ = 20 W, and these values remain constant through the analysis. In Fig.2, $\dot{Q}_{ref.g}$ and $\dot{Q}_{ref.l}$ are refrigeration loads absorbed by the heat exchanger in the gas and liquid region, respectively. Table 1 shows a summary of mass and energy balance equations for control volumes of gas and liquid region, and selected natural convection heat transfer correlation.

Liquefaction Model

The in situ liquefaction is performed at a constant tank pressure, P, while the LN_2 precooled hydrogen gas ($\dot{m}_{in}$) flows into the tank to compensate for the condensed gaseous hydrogen to liquid ($\dot{m}_{cond}$) and maintain the pressure. At near-ambient tank pressure, gaseous hydrogen in the gas region can be considered as an ideal gas. In the liquid region, LH_2 is considered as an incompressible liquid. By applying the ideal gas conditions for gaseous hydrogen and incompressible

Table 1. Mass, energy balance and natural convection heat transfer correlation for gas and liquid hydrogen regions.

Liquefaction model	Densification model
$\frac{dm_g}{dt} = \dot{m}_{in} - \dot{m}_{cond}$	$\frac{dm_g}{dt} = -\dot{m}_{cond}$
$\frac{d(m_g u_g)}{dt} = \dot{m}_{in} h_{in} - \dot{m}_{cond} h_l + \dot{Q}_{w.g} + \dot{Q}_{manway} - \dot{Q}_{ref.g}$	$\frac{d(m_g u_g)}{dt} = -\dot{m}_{cond} h_l + \dot{Q}_{w.g} + \dot{Q}_{manway} - \dot{Q}_{ref.g}$
$\frac{dm_l}{dt} = \dot{m}_{cond}$	$\frac{dm_l}{dt} = \dot{m}_{cond}$
$\frac{d(m_l u_l)}{dt} = \dot{m}_{cond} h_l + \dot{Q}_{w.l} + \dot{Q}_{support} - \dot{Q}_{ref.l}$	$\frac{d(m_l u_l)}{dt} = \dot{m}_{cond} h_l + \dot{Q}_{w.l} + \dot{Q}_{support} - \dot{Q}_{ref.l}$

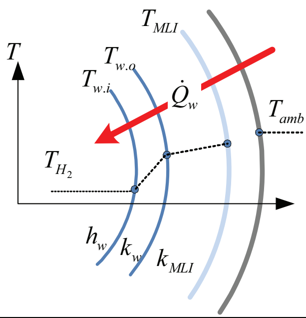

$$Nu = \frac{h_w \cdot k_{H_2}}{D_{tank}} = 0.555\ Ra^{1/4} \quad \text{for laminar}$$

$$Nu = \frac{h_w \cdot k_{H_2}}{D_{tank}} = 0.0210\ Ra^{2/5} \quad \text{for turbulent}$$

$$\text{where, } Ra = Gr \cdot Pr, \quad Gr = \frac{g\beta\left(T_w - T_{H_2}\right) D_{tank}{}^3}{\nu^2}$$

fluid condition for liquid hydrogen, mass and energy balance equations are reduced to the following equations.

$$\dot{m}_{cond} = \frac{\dot{Q}_{ref.g} - \dot{Q}_{w.g} - \dot{Q}_{manway}}{\left(h_{in} - h_l\right) + \frac{\rho_g}{\rho_l} u_g} \tag{1}$$

$$\dot{m}_{in} = \dot{m}_{cond}\left(1 - \frac{\rho_g}{\rho_l}\right) \tag{2}$$

Densification Model

When the storage tank contains a certain level of LH_2, densification can be demonstrated by closing the hydrogen inflow valve while the refrigerator runs continuously at lower temperature than NBP of hydrogen. In this case, the heat exchanger condenses gaseous hydrogen to liquid and densifies the liquid hydrogen below NBP at the same time. As a result, the tank pressure drops due to the condensation in the gas region, and also due to the reduced liquid temperature. As in the Liquefaction model, gaseous hydrogen can be treated as an ideal gas with constant temperature (T_g), but the tank pressure varies in the densification model. Also, liquid hydrogen can be considered as an incompressible fluid, but its pressure and temperature (T_l) are not constant in this case. Applying these assumptions into the equations in Table 1, mass and energy balance equations are reduced to the following equations.

$$\dot{m}_{cond} = \frac{\dot{Q}_{ref.g} - \dot{Q}_{w.g} - \dot{Q}_{manway}}{u_g - h_l} \tag{3}$$

$$\frac{dT_l}{dt} = \frac{1}{m_l C_l}\left[\dot{Q}_{support} + \dot{Q}_{w.l} - \dot{Q}_{ref.l} + \dot{m}_{cond}\left(h_l + u_l\right)\right] \tag{4}$$

$$\frac{dP}{dt} = \frac{\dot{m}_{cond} R T_g}{V_g}\left(\frac{P}{\rho_l R T_g} - 1\right) \tag{5}$$

Equation (3)~(5) are numerically integrated with given initial conditions, for example, initial storage tank pressure, liquid level, and the refrigerator performance curve as a function of cooling temperature. As convergence criteria, the following simple equations can verify convergence of the numerical scheme.

$$\dot{Q}_{ref} = \dot{Q}_{ref.g} + \dot{Q}_{ref.l} \tag{6}$$

$$P = P_{sat}\left(T_l\right) \tag{7}$$

In order to estimate heat leaks through the tank walls, $\dot{Q}_{w.g}$ and $\dot{Q}_{w.l}$, a set of mass and energy balance equations for the tank wall, MLI, and outer wall were combined with those of hydrogen, and were numerically solved at the same time to simulate thermal equilibrium of hydrogen regions and the tank walls. The natural convection heat transfer coefficient correlations in Table 1, the wall dimensions, and MLI specifications were adopted from previous analysis.[3,7-8]

The inner storage tank shape was simplified to a horizontal cylindrical double walled SUS304 vessel with zero dish head fraction in the models. The inner storage tank dimensions are 2.896 m in diameter, 20.3 m in length, and 12.7 mm of wall thickness.

RESULTS AND DISCUSSION

Liquefaction

Before the liquefaction begins, the storage tank walls are precooled to 78K with LN_2 and the tank is filled with gaseous hydrogen at the same temperature. The Linde R1620 produces 800 W of net refrigeration power at 20 K including connecting lines losses.[3] The tank pressure remains the same through the liquefaction. The heat exchanger in the tank condenses 78 K gaseous hydrogen into 20 K (or saturated temperature at a given liquefaction pressure) liquid hydrogen. Initially, the condensed liquid cools down the bottom tank walls until the wall temperature reaches near 20 K. The evaporated gaseous hydrogen is re-condensed to liquid, and eventually liquid starts accumulating in the tank bottom. The precooled gaseous hydrogen flows into the tank to make up the condensed hydrogen mass as the liquefaction progresses. After continuing these processes over time, the liquid level increases in the storage tank.

First, the liquefaction simulation was performed at a constant pressure of 1 bar to validate the heat transfer coefficient correlation and other modeling assumptions. After thermal equilibrium among hydrogen, the tank walls and MLI was reached, the converged values for natural convection heat transfer coefficients in the gas region and liquid region, $h_{w.g}$ and $h_{w.l}$ were 4 and 30 W/m^2-K, respectively, for 1 bar, 20 K liquefaction. The storage tank wall temperatures were close to that of the liquid within a 1 K offset. Also, the temperature difference between the inside and outside of the inner wall was less than 1 K for both the gaseous and liquid regions. Regarding condensation efficiency on the heat exchanger surface, typical condensation heat transfer coefficients for hydrogen have been reported to be 100~200 W/m^2-K.[9] Considering the maximum heat exchange surface of 8 m^2 with the pre-estimated available refrigeration power for liquefaction of about 500 W[3], the assumption of ideal condensation at the heat exchanger seems to be reasonable.

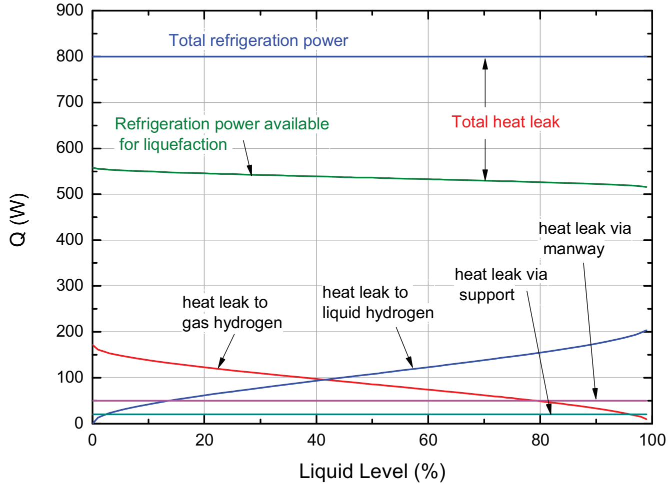

Figure 3. Heat leak distribution and available refrigeration power for liquefaction as a function of liquid hydrogen level in the storage tank.

Figure 3 shows heat leak distributions in the gaseous and liquid region and available refrigeration power for liquefaction as a function of liquid level percent in the tank. The liquefaction simulation continued for various pressures to see the effect of pressure. At the beginning of liquefaction (i.e., liquid level= 0%), a major heat leak occurs at the 78 K wall as expected. At around 42% liquid level, heat leaks through the gaseous and liquid region walls become the same. As the liquid level becomes higher, available refrigeration power for liquefaction becomes less. When the tank is full of liquid hydrogen, total heat leak was estimated to total 284 W including auxiliary losses. This value is fairly comparable to the KSC's first calorimetric heat leak testing result, 300 W. The difference of estimated total heat leaks is due to higher MLI performance assumption in this simulation. At the 50% liquid level, liquefaction rate ($\dot{m}_{cond}$) and compensation inflow rate ($\dot{m}_{in}$) are 0.503 g/sec and 0.501 g/sec (or 372 SLPM), respectively.

The liquefaction simulation continued for various liquefaction pressures to see the effect of increased saturation temperature on liquefaction rate. One can expect a higher liquefaction rate at higher liquid temperature with given refrigeration power. Liquefaction time required to fill up the storage tank to a specific liquid level is also a valuable operational parameter for planning the testing schedule. The liquefaction rates were numerically integrated over time for various liquefaction pressures. Figure 4 shows the required liquefaction time profiles to obtain a specific liquid level at various liquefaction pressures. In order to liquefy the 78 K 100% gaseous hydrogen to 20 K liquid hydrogen to 100% fill level, the GODU LH_2 will take about 210 days with the current refrigerator cooling capacity. If the liquefaction begins with existing liquid hydrogen level in the tank, total liquefaction time will be significantly reduced, and the new time profiles can be easily estimated from this model.

Densification

In general, the net available refrigeration power decreases as refrigeration temperature decreases. From the manufacturer performance validation results, the Linde R1620 produces 400~420 W of refrigeration power at 17 K. The densification begins at a given liquid level without gaseous hydrogen feeding flow into the storage tank. Depending upon the initial liquid level in the tank, the refrigeration power distribution in the gaseous and liquid hydrogen region will vary due to different heat leaks and the tank wall temperatures in the gaseous and liquid regions. Also, heat leaks to the storage tank will increase due to lower LH_2 temperature and as a result, the tank wall temperatures as well.

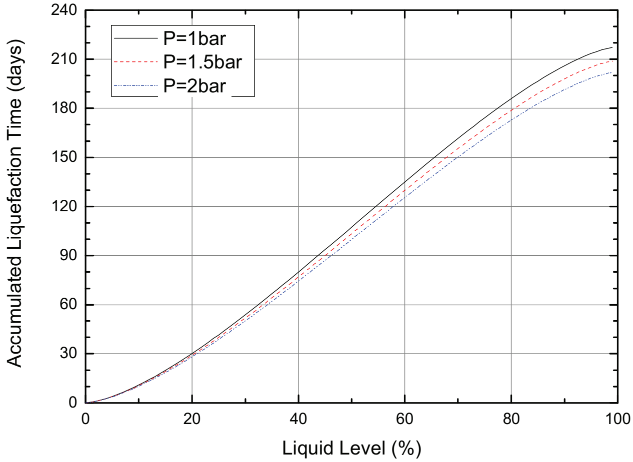

Figure 4. Required liquefaction time as a function of liquid level at various pressures.

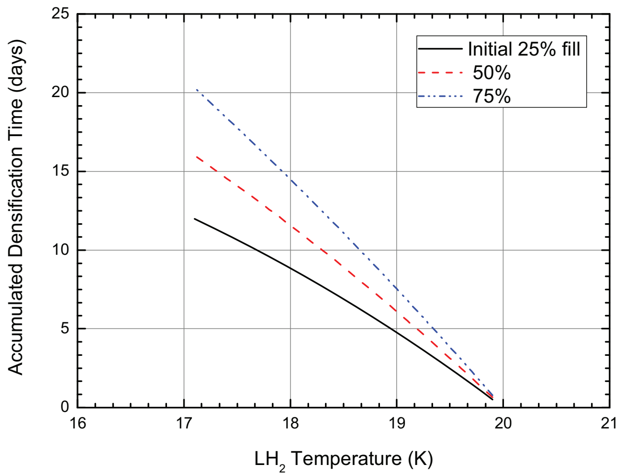

Figure 5. Transient LH_2 temperature profiles during densification for various initial fill levels.

Figure 5 shows the transient LH_2 temperature change profiles during densification for various initial fill levels when the refrigerator continuously runs at 17 K. As the initial fill level before the densification increases, total densification time required increases due to the increase of thermal cooling mass. The required densification time is one order of magnitude shorter than that of liquefaction mode. From Figs. 4 and 5, one can easily estimate the required liquefaction time to a specific liquid level, total required densification time from a specific fill level, and transient fluid condition at any given time during each process.

The total heat leak to the storage tank doesn't decrease significantly as the LH_2 temperature decreases below NBP. For example, at a 75% fill level, the total heat leak to 20 K and 17 K LH_2 are 272 W and 280 W, respectively. On the other hand, the available refrigeration power significantly drops between these two temperatures.

During the densification process, a certain amount of gaseous hydrogen is condensed by the heat exchanger in the gaseous region, and it increases the liquid level. For example, at the 25% fill level, initial total hydrogen mass in the tank is 1901 kg, and the mass condensed during the densification is 81 kg. This results in a 4.26% increase in liquid volume during the densification. The liquid volume increase percentage decreases as the initial fill level increases due to less ullage volume in the tank. For the 75% fill level, the initial total hydrogen mass is 7616 kg and the mass condensed in the gaseous region is 19.7 kg which is less than 1.6% in liquid level increase. This information will be useful to estimate ullage volume changes of the tank, and to determine tank pressurization and transfer operation parameters in various operation modes.

CONCLUSION

The NASA KSC is in the process of modernizing liquid hydrogen systems to optimize life cycle costs for the unique KSC application. As a part of the efforts, the GODU LH_2 will demonstrate state-of-the-art cryogenic propellant handling techniques to enhance overall spaceport economics with many environmental benefits. A thermal analysis with lumped model was performed for the GODU LH_2 to predict thermal losses, fluid conditions, and operational time for advanced LH_2 handling and conditioning. The analysis estimated overall thermal losses and transient behavior of the storage tank during the in situ hydrogen liquefaction and densification operation modes. The analysis results are practically useful for the GODU LH_2 researchers to understand system behaviors and predict propellant conditions in various operational modes.

ACKNOWLEDGMENT

This research was supported by the Converging Research Center Program funded by the Ministry of Education, Science and Technology in Korea (2013K000409).

REFERENCES

1. Partridge, J.K., “Fractional Consumption of Liquid Hydrogen and Liquid Oxygen during the Space Shuttle Program,” *Advances in Cryogenic Engineering*, AIP Conference Proceedings, Vol.1434 (2012), pp. 1765-1770.
2. Notardonato, W.U., Johnson, W.L., Oliveira, J. and Jumper, K., “Experimental Results of Integrated Refrigeration and Storage System Testing,” *Advances in Cryogenic Engineering*, AIP Conference Proceedings, Vol.1218 (2010), pp. 1369-1376.
3. Fesmire, J.E., Tomsik, T.M., Bonner, T., Oliveira, H.J., Conyers, H.J., Johnson, W.L. and Notardonato, W.U., “Integrated Heat Exchanger Design for a Cryogenic Storage Tank,” *Advances in* Cryogenic *Engineering*, AIP Conference Proceedings, Vol.1573 (2014), pp. 1365-1372.
4. Johnson, R.G., Notardonato, W.U., Currin, K.M., and Orozco-Smith, E.M., “Integrated Ground Operations Demonstration Units Testing Plans and Status,” *AIAA Space 2012 Conference and Exposition* (2012), Pasadena, California.
5. Baik, J.H., and Notardonato, W.U., “Initial Test Results of Laboratory Scale Hydrogen Liquefaction and Densification System,” *Advances in* Cryogenic *Engineering*, AIP Conference Proceedings, Vol.823 (2006), pp.1530-1537.
6. Baik, J.H., Karng, S.W., Carceau, N., Jang, Y.H., Lim, C.M., Kim, S.Y., and Oh., I., “Development of 1 L/hr Scale Hydrogen Liquefier Using Gifford-McMahon (GM) Cryocooler,” *Advances in Cryogenic Engineering*, AIP Conference Proceedings, Vol.1573 (2006), pp. 1357-1364.
7. Oliveira, J.M., Kirk, D.R., and Schallhorn, P., “Analytical Model for Cryogenic Stratification in a Rotating and Reduced-Gravity Environment,” *Journal of Spacecraft and Rockets*, Vol. 46, No. 2 (2009), pp. 459-465.
8. Jesmire, J.E., Coffman, B.E., Meneghelli, B.J., and Heckle, K.W., “Spray-on Foam Insulations for Launch Vehicle Cryogenic Tanks,” *Cryogenics*, Vol. 52 (2012), pp. 251-261.
9. Frost, W., *Heat Transfer at Low Temperatures*, Plenum Press, NY and London (1975), pp. 209.